# New Optical Detector Concepts for Space Applications

D. A. Cardimona, D. H. Huang, D. T. Le, T. Apostolova, P. M. Alsing, W. Glass, and C. D. Castillo
Air Force Research Laboratory, Space Vehicles Directorate
3550 Aberdeen Ave., S.E., Kirtland AFB, NM 87117-5776

## ABSTRACT

In the Advanced Detectors Research Group of the Air Force Research Laboratory's Space Vehicles Directorate, we work to enhance existing detector technologies and develop new detector capabilities for future space-based missions, most often using photonic techniques. To that end, we present some ideas we are presently investigating: (i) tuning the wavelength response of detectors using applied electric or magnetic fields, (ii) detecting the full polarization vector of a signal within a single pixel of a quantum well detector, (iii) monolithic solid-state cooling of a detector using photoluminescence, and (iv) enhancement of weak electromagnetic fields using interactions with plasmons.

Keywords: QWIP, quantum well, infrared, tunable detection, polarization, solid state cooling, laser cooling, photoluminescent cooling, plasmon, plasmonics, near-field enhancement

## 1. INTRODUCTION

Photonics is the technology of generating and/or harnessing photons for use in controlling, manipulating, transferring, and/or storing information. The science of photonics includes the emission, transmission, deflection, amplification, and detection of photons. Therefore, photonics technologies play a major role in surveillance, reconnaissance, and situational awareness systems in space. Desired sensing capabilities for these space systems include: dim or distant object detection and identification through multicolor or polarization sensing, the ability to reconfigure for multiple missions, day and night remote sensing of near and far objects that could be hot or cold, the ability to discriminate small features, the ability to determine mass or status of unknown objects, the ability to sense with a wide field of view, etc. In addition to these wonderful capabilities, the sensors in space systems must operate in a radiation environment, must have low noise due to the weak signals and extremely low photon backgrounds, and usually must be cooled (if the sensing wavelength is in the infrared). Photonics technologies provide methods to acquire all of these capabilities.

In the following, we will describe some of our photonic research efforts here at the Air Force Research Laboratory's Space Vehicles Directorate in tuning the wavelength response of a detector, sensing the full polarization vector within a single pixel of a detector, cooling a detector without using any moving parts, and enhancing an input optical signal.

## 2. LATERAL BIASING FOR TUNING THE DETECTED WAVELENGTH

One sensor feature that enables object discrimination and identification is the ability to determine the exact spectral signature of the object. Currently, this feature is implemented using spectral filters and multiple focal plane arrays (FPAs), each with its own set of optical elements. Bandgap-engineered semiconductor quantum well infrared photodetectors (QWIPs), as well as quantum dot infrared photodetectors (QDIPs) have been shown to exhibit a voltage-tuning capability where the spectral response of a single device can be "tuned" when a bias voltage applied across the growth layers (parallel to the growth direction) is varied. This voltage tuning is produced by the quantum-confined Stark Effect – the shifting of quantized energy levels due to an applied electric field. Voltage tunability can be used to determine the exact spectral signature of an object, without the use of spectral filters or multiple FPA channels. This could result in a significant reduction in the complexity, cost, and weight of the sensor.

The above so-called vertical biasing is not the only possibility. We can also apply a bias field laterally across the pixel, parallel to the plane of the quantum wells (perpendicular to the growth direction). In this case, we first design an asymmetric double quantum well (DQW) structure with a thin middle barrier between the two wells. In this asymmetric DQW structure, a narrow well doped with electrons contains a ground state and an excited state, while a step-lifted wide undoped well contains only one state, resonant with the excited state in the narrow well. The most important innovation

Photonics for Space Environments X, edited by Edward W. Taylor, Proceedings of SPIE Vol. 5897
(SPIE, Bellingham, WA, 2005) · 0277-786X/05/$15 · doi: 10.1117/12.613654

of this DQW structure is that the two quantum wells can be independently biased laterally from the sides of the pixel, so that planar transport instead of vertical transport can occur in the individual wells and can be controlled independently. The step up to the wide well will be used to reduce the dark current when it is biased laterally. When the electrons in the narrow quantum well absorb a photon, they can transit to the upper excited state in the same well and then rapidly move into the wide well through the resonant tunneling process due to the thin barrier between these two wells. Consequently, the electrons in the wide well will be swept to the collector region when the lateral bias is applied to this well. Because the photo-excited electrons are driven by the lateral bias in one of the quantum wells, a unit optical gain is expected due to the lack of carrier capture processes during transport (compared to 20% or less in vertically-biased QWIPs).

## 3. POLARIZATION DETECTION WITHIN A SINGLE PIXEL

An imaging polarimeter captures an image with both the intensity and the average polarization state recorded for each pixel. A polarimetric image has more information than a simple intensity image and improves remote sensing and automatic target recognition. Polarimetry can be used to identify materials and to distinguish samples from a cluttered background. Polarimetry has also shown promise for mine detection, contrast enhancement, and shape determination. On average, polarimetric images of man-made objects have a higher degree of polarization than polarimetric images of natural objects. This pattern could be useful for spectro-polarimetric sub-pixel target detection. All current polarimeters create multiple images with different polarizing filters. If the polarization is determined using simultaneous images on different focal planes, spatial resolution errors occur. If the polarization is determined using several consecutive images with a single focal plane, temporal registration errors will occur.

We have invented a scheme that should alleviate each of the errors mentioned above. In our device, four quantum-well stacks are used in combination with linear gratings aligned in different direction to determine the degree of polarization of incident light within a single pixel. The quantum well stacks do not absorb light having an electric field component parallel to the stacks (due to quantum mechanical selection rules). The non-absorbed propagating light is reflected, diffracted, and transmitted at each grating as a function of its polarization. Interference translates the incident polarization into the amount of polarized light having an electric field with a component in the z-direction. This z-polarized component of the light is absorbed by the quantum wells. The photocurrent from each quantum-well stack is read out separately. The voltage bias across each stack is individually adjusted, and the photocurrent is proportional to the flux of light absorbed by that quantum-well stack.

In order to validate the principle-of-operation described above, we developed a working electromagnetic model of the device using transfer-matrix techniques.[1] Figure 1 shows the fraction of incident light absorbed in the four quantum-well stacks versus the angle of linearly polarized incident light. These curves demonstrate that the relative photocurrents from the four quantum-well stacks provide a means to measure the polarization of incident light.

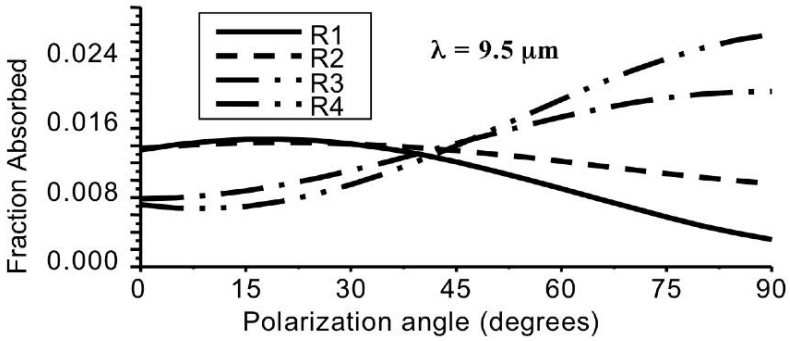


**Figure 1:** An example of the response from the four layers of the pixel-polarimeter as we rotate the polarization angle of the incident linearly-polarized light.

The next challenge was to find a process that would allow the fabrication of the device. We began with a proof-of-concept two-layer test structure. We used a wafer fusion approach to create the various layers of quantum wells and gratings. For the two-layer device, the quantum wells were each grown on a perfect substrate and one set of gratings was

etched on one wafer. A second wafer was then fused to the grating surface of the first wafer by Dr. Liau's group at the MIT Lincoln Laboratory, using a method they developed.[2] The top substrate was then removed and a second layer of gratings was etched on top. The final structure is shown in Fig. 2. This structure was then prepared for characterization, however there are some processing problems that need to be overcome for our next attempt at this proof-of-concept pixel-polarimeter. This figure actually shows a hole that was created when a contact was ripped off by accident.

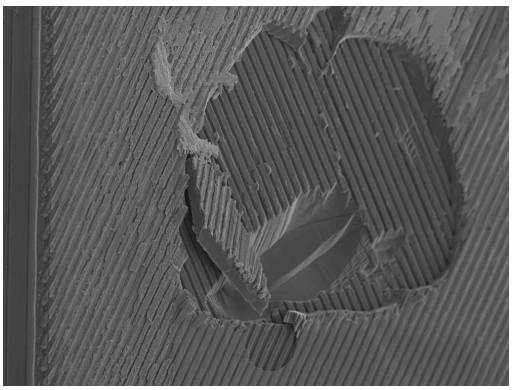

**Figure 2:** This is an SEM of our first attempt at a proof-of-concept, two-grating-layer pixel polarimeter. Pictured is a top layer of gratings, then a layer of quantum well material, then another layer of gratings, another layer of quantum well material, and a substrate.

## 4. PHOTOLUMINESCENCE ("LASER") COOLING OF SOLIDS

Infrared photodetectors generally need to be cooled in order to work more efficiently. There are several approaches to cooling solid-state detectors, including mechanical cooling, thermoelectric cooling, thermionic cooling, opto-thermionic cooling, and fluorescent cooling. Some of these cooling concepts provide very attractive possibilities for cryogenics-on-a-chip, either including contacts for a current flow under a bias or excluding contacts by replacing the bias with a resonant optical field. Solid state cooling will have many advantages for space-based sensing missions. Such a cooler will have no vibration to contend with. It should be free of electronic, magnetic, and electromagnetic noise. With no moving parts, it should have a very long lifetime. The solid-state cooling technologies are accomplished with low-cost materials and manufacturing, and should be highly reliable. A complete solid-state cryocooler with a cubic centimeter of volume (and in some cases, much less than that) seems possible. This extreme miniaturization could lead to cooling a focal plane array, pixel by pixel.

The cooling of a solid via light-induced fluorescence has been of interest for a very long time.[3] This interesting phenomenon involves the excitation of an electron from the valence bandedge to the conduction bandedge by absorbing a pump photon (see Fig. 3).

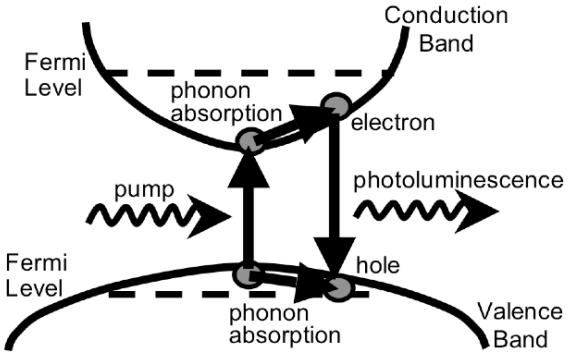


**Figure 3:** This is a band diagram of the photoluminescence cooling mechanism in semiconductors.

This cool electron quickly becomes hot by gaining thermal energy through ultrafast electron-phonon scattering. After a radiative lifetime, recombination of the hot electron will produce a spontaneous photon with energy higher than that of the pump photon. As a result, the lattice will be cooled due to the loss of thermal energy to the electron. It is only recently that this phenomenon has been observed experimentally. Laser-induced fluorescent cooling of heavy-metal-fluoride glass doped with trivalent ytterbium ions was the first realization of this concept.[4] Soon to follow were demonstrations of cooling in dye solutions[5] and thulium-doped glass.[6]

Laser cooling of a semiconductor, however, remains an elusive goal, although it has been pursued for many years. The key question we have tried to answer is: what are the best semiconductor materials and conditions for achieving the greatest laser cooling effect? This requires an accurate *nonlocal* theory on a microscopic level, which directly provides an evolution equation for the lattice temperature by including the dynamical effects. We have developed such a *nonlocal* theory for the laser cooling of semiconductors.[7] By including the effect of the carrier distribution, we were able to uncover the essential physics underlying the phenomenon and we provided important quantitative predictions that can guide experimentalists toward achieving maximum efficiency of laser cooling in the future.

We assumed a weak pump laser first excites electrons from the valence bandedge to the conduction bandedge. The excited carriers instantaneously form a nonequilibrium distribution. It is well known that the quantum kinetics of the scattering of electrons with phonons or other carriers under a weak pump field can only be seen within the time scale of several hundred femtoseconds. Subsequently, ultrafast carrier-phonon and carrier-carrier scattering quickly adjusts the kinetic energies of these excited carriers by taking energy from the lattice. As a result, a quasi-equilibrium Fermi-Dirac distribution of carriers is formed in about 0.1 ps, with an electron temperature determined by the pump-field intensity, pump-photon energy, and lattice temperature. After a few tens of nanoseconds, radiative decay of the excited carriers will begin to affect the electron distribution. The electron temperature will be adiabatically readjusted according to an energy balance between the power-gain density due to optical absorption, the power-loss density due to photoluminescence, and the power-exchange density due to scattering with phonons. At the same time, the lattice temperature will evolve because of an imbalance between the power loss due to transferring phonon energy to carriers and the slight power gain from the external thermal radiation. Just before the radiative decay occurs, the lattice and the electrons are in thermal equilibrium with an initial temperature which can be determined by solving a semiconductor Bloch equation.

Using this nonlocal theory, we found that the laser-cooling rate is largest for a large bandgap material, a weaker pump-laser field, and a high initial lattice temperature (see Fig. 4). We also found that the laser-cooling power decreases as the lattice cools down.

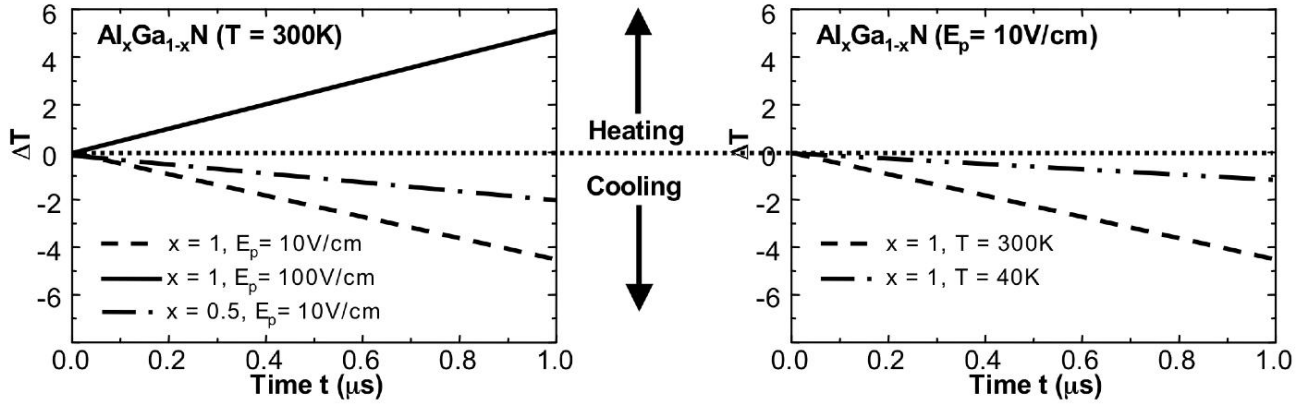


**Figure 4:** The graph on the left indicates that there is greater cooling for lower pump power and wider bandgap. The graph on the right indicates that there is greater cooling when the initial temperature is higher.

## 5. LASER COOLING OF SEMICONDUCTOR QUANTUM WELLS

We have generalized our above theory to a microscopic theory for spatially-selective laser cooling in undoped semiconductor quantum wells, which cools the part of the lattice inside the well region more than that outside the well in the barrier region.[8] Our model is based on the following four successive physical steps: (i) photo-excited cold carriers with nearly-zero kinetic energies are coherently and resonantly excited across a bandgap by a weak laser field; (ii) the photo-induced cold carriers in conduction and valence bands are heated to higher energy states above their chemical potentials via inelastic phonon scattering; (iii) the hot electrons and holes recombine through radiative decay giving rise to fluorescent photons, thus taking away more power from the quantum-well system than that acquired through the laser-field absorption; (iv) phonons in the system thermally diffuse into the central cool region (quantum well) from two surrounding warm regions (barriers), thereby allowing the entire lattice to cool below the thermally-isolated surrounding environment.

It has been known for a long time that the exciton effect at room temperature becomes negligible in GaAs quantum wells. However, the interaction between electron and hole plasmas is still expected to play a major role during the second step of the four-step laser cooling model. The resulting detailed balance between interacting electron and hole plasmas (due to carrier-carrier scattering) locks the carrier temperatures to a common value $T(z)$. The strong confinement of the photo-induced carriers within the quantum wells prevents carriers from diffusing in the $z$ direction perpendicular to the quantum wells. Since the time for the carriers to adjust their temperature is much shorter than the evolution time of the lattice temperature, the conservation of total energy of confined electrons and holes gives rise to a detailed-energy-balance equation at each $z$ position during the last step of the four-step model. This energy-balance equation can be used to adiabatically determine the spatial dependence of the carrier temperature $T(z)$ for each profile of the lattice temperature $T_L(z)$. The slow time evolution of the lattice-temperature profile $T_L(z)$ during the last step of the model is found to be determined by a thermal-diffusion equation for phonons. The carrier temperature will be thermally dragged down by the reduction of the lattice temperature with time.

In the lefthand graph of Fig. 5, when the lattice temperature is high (of the order of 300K) and inelastic phonon scattering of photo-excited carriers is very effective and dominated by LO phonons, a dip in the z-dependent temperature appears in the well within a few radiation lifetimes (nanoseconds) after the pump is turned on. As cooling progresses, the dip increases at well-center for a while. On the right of Fig. 5, we see that when the lattice temperature reaches very low values (around 40K) where phonon diffusion is less prevalent and scattering is dominated by LA and TA phonons, the central temperature dip tends to flatten out. Finally, the entire lattice (well and barrier) reaches a uniform value.

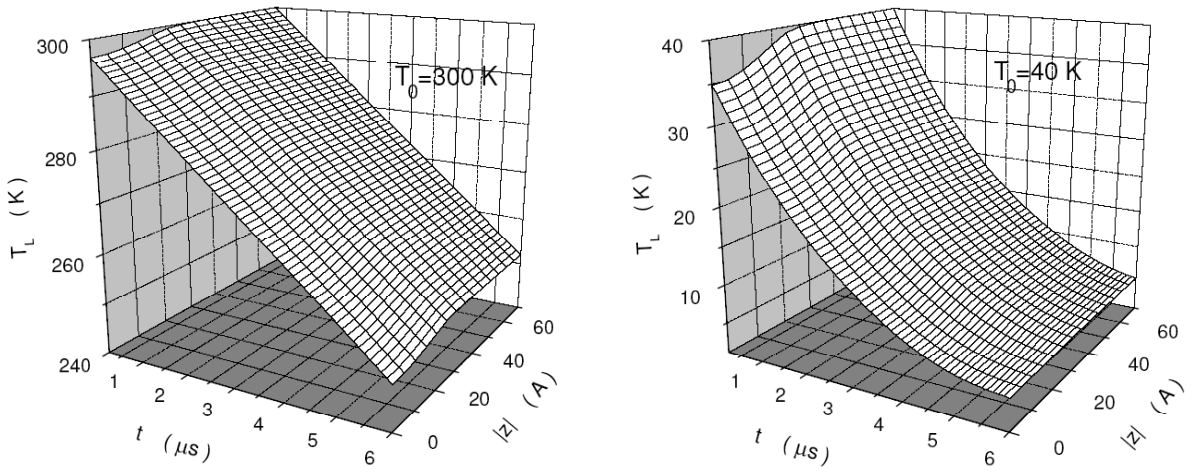


**Figure 5:** These are graphs of lattice temperature versus time and position. On the left we see the increase of the central dip at higher temperatures. On the right we see the flattening of the temperature profile at lower temperatures.

## 6. OPTICAL SIGNAL AMPLIFICATION WITH PLASMONICS

A plasmon is a quantized electron density wave in a conducting material. Bulk plasmons are longitudinal excitations, whereas surface plasmons (SPs) can have both longitudinal and transverse components. Light of frequency below the frequency of the plasmon for that material (the plasma frequency) is reflected, while light above the plasma frequency is transmitted. SPs on a plane surface are non-radiative electromagnetic modes, that is, they cannot be generated directly by light nor can they decay spontaneously into photons. However, if the surface is rough, or has a grating on it, or is patterned in some way, light around the plasma frequency couples strongly with the surface plasmons, creating what is called a polariton, or a surface plasmon polariton (SPP). An SPP is a localized, coupled electromagnetic field/charge-density oscillation, which may propagate along an interface between two media. Another way to create an SPP is to couple the incident light into the plasmon via frustrated total internal reflection. SPs play a role in surface-enhanced Raman scattering. When they couple to the incident light, they can actually enhance the electric field in the near field (the evanescent field).

Very recently, Ebbesen *et al.*[9] have reported on enhanced optical transmission seen in arrays of subwavelength cylindrical holes in metallic films. Similar phenomena have also been observed in subwavelength metallic gratings[10] and even in simple planar metallic films.[11] These enhanced optical transmissions are believed to be related to light coupling to surface-plasmon-polaritons in non-structured or structured metallic films. For a very thin metallic film with thickness less than both the incident wavelength and the absorption length of the metal, only one two-dimensional (2D) gapless plasmon mode exists. For a thick metallic film, on the other hand, a 3D plasmon mode with a gap can exist, in addition to the existence of surface-plasmon-polariton modes. For semi-infinite metals, two surface-plasmon modes can exist.

In order to understand the physics involved in the enhanced optical transmission, near-field calculations are preferred. There are three common ways to describe the metal optical properties. The first is to assume a perfect conductor inside which the electric field is zero. The second is to model the metal as a dispersive material with a momentum-independent dielectric function. The last is to model the metal as a dissipative material with a simple Drude-type dielectric function. We feel that none of these three models can be applied to metallic films in a general fashion. Our argument is as follows: (1) If the skin depth becomes larger than the thickness of the metallic film, the assumption of a perfect conductor is no longer valid; (2) If the incident light is either diffracted or scattered by some surface structures on the surface of the metallic film, the momentum-independent dielectric function is no longer applicable to high-order diffracted fields; (3) When the frequency of the incident field is close to the 3D plasma-wave frequency of the metal, the effect from a nonlocal 3D plasma wave must be included with a momentum-dependent dielectric function.

We studied a unique structure composed of a half-space of air and a doped semi-infinite GaAs bulk covered by a heavily-doped InAs conducting interface sheet, from which the physics behind the resonant coupling between 3D and 2D plasma-wave excitations and the effect of evanescent modes can be explored. The reason for choosing the doped InAs instead of a metal is that variable doping density and the homogeneous broadening in InAs is much smaller than that in a metal, which ensures the resonant coupling between 3D and 2D plasma-wave excitations. The inclusion of a doped GaAs bulk allows for both surface and 3D plasma waves[12] in addition to the 2D plasma wave existing in the InAs conducting sheet. The presence of both 3D and 2D plasma waves enables the longitudinal and transverse electromagnetic oscillations to couple in directions both perpendicular and parallel to the sheet. We have developed a spatially-nonlocal dynamic theory in order to determine the transmissivity of an electromagnetic wave incident on our proposed structure.[13] With this structure, we explored the physics behind the resonant coupling between 3D and 2D plasma-wave excitations due to induced current and material polarization within the sheet and the effect of evanescent modes. We also investigated effects due to strong interactions between excited carriers and incident photons.

In addition to several effects due to resonant coupling between 2D and 3D plasma-wave excitations, we predict an evanescent-mode-enhanced optical transmissivity by the doped semi-infinite GaAs bulk (see Fig. 6).

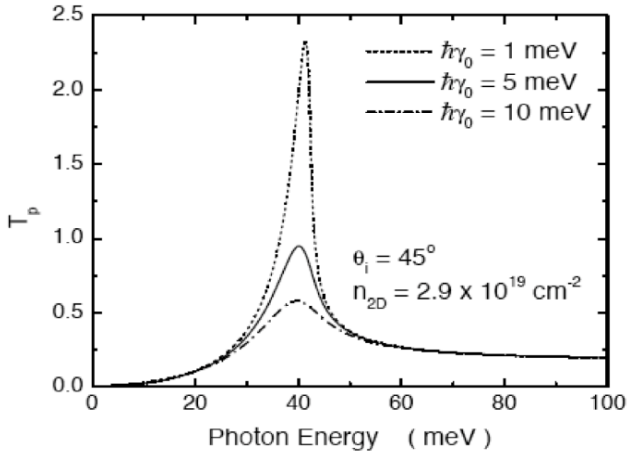


**Figure 6:** This graph shows how the transmission is enhanced in the near field as the plasmon lifetime decreases (i.e., as the amount of electron scattering increases).

The evanescent-mode-induced near-field enhancement can be used to increase the sensitivity of quantum detectors buried just below the bulk surface, including quantum-well, quantum-wire and quantum-dot detectors, since their photoresponse depends only on the *E*-field and not on the *H*-field component[14] (see Fig. 7).

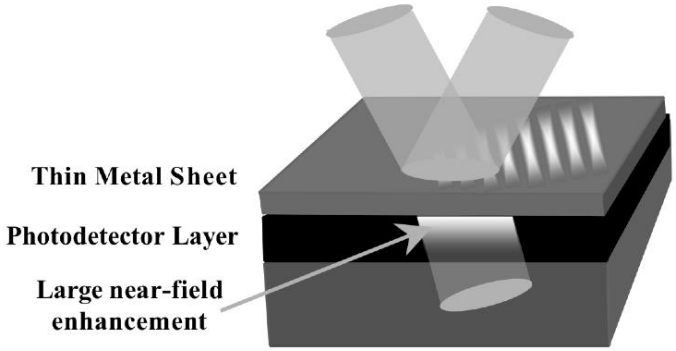


**Figure 7:** This is a representation of a concept for amplifying an incoming optical signal in a layer of detector material, using plasmonic interactions to enhance the near-field transmission through a metal film.

The evanescent-mode-induced enhancement does not violate energy conservation since these modes do not carry any net energy. For the near-field angular distribution, the presence of the InAs conducting sheet on top of the doped GaAs bulk enhances the transmitted *E*-field for *s* polarization but leaves the transmitted *E*-field almost unchanged for *p* polarization. The enhancement of the transmitted *E*-field in our structure is predicted to be as large as ten times greater than that obtained with an InAs conducting sheet on an undoped GaAs bulk.

## 7. SUMMARY AND CONCLUSIONS

A wavelength-tuning capability in an IR sensor will provide the ability to successfully perform missions involving space-based intelligence and surveillance such as detection and identification of biological and chemical weapons storage and/or production facilities, and detection, identification, and tracking of tactical and strategic missiles during and after launch. Many space situational awareness missions will also be enabled by such a capability. If all of these various missions could be performed by a single, reconfigurable sensor system, the cost savings would be enormous. We have described one possible approach to attaining this goal: the lateral biasing of a quantized detector.

A polarization-detection capability will also provide additional information to any surveillance system. At the very least, it could provide the ability to queue higher resolution sensor systems when interesting polarization signatures are detected. We have described a new photonic device that promises to detect, simultaneously and instantaneously, the full polarization state of an incident signal within each pixel of a photodetector array. Other techniques for capturing polarimetric images involve large errors at the edges of objects in the scene or require the designer to sacrifice spectral resolution or increase the weight by using beam splitters and multiple focal plane arrays. This device uses the selective absorption properties of quantum well detectors.

We have described the "new" (only in the sense of now it might be able to be accomplished) solid-state cooling scheme called laser cooling. This cooling mechanism could lead to an extreme miniaturization of the cooling system, for on-chip, pixel-by-pixel cooling. This sort of cooling system is vibration and noise free, should be very reliable and robust, should have a long lifetime, and should be very low in cost.

Finally, we have described how surface plasmon polaritons that arise when electromagnetic fields couple to thin metal sheets might be used to enhance input signals in the near field. We envision placing a photodetector that responds to the electric-field component of an incident electromagnetic field within this enhanced near-field, thereby improving the detection prospects for very weak signals due to dim or distant objects.

## REFERENCES


1. M. Serna, Inf. Phys. & Tech. **44**, 457 (2003).
2. Z. L. Liau and D. E. Mull, Appl. Phys. Lett. **56**, 737 (1990).
3. P. Pringsheim, Z. Phys. **57**, 739 (1929).
4. R. I. Epstein, M. I. Buchwald, B. C. Edwards, T. R. Gosnell, and C. E. Mungan, Nature **37**, 500 (1995).
5. J. L. Clark and G. Rumbles, Phys. Rev. Lett. **76**, 2037 (1996).
6. C. W. Hoyt, M. Sheik-Bahae, R. I. Epstein, B. C. Edwards, and J. E. Anderson, Phys. Rev. Lett. **85**, 3600 (2000).
7. D. H. Huang, T. Apostolova, P. M. Alsing, and D. A. Cardimona, Phys. Rev. B **70**, 033203 (2004).
8. D. H. Huang, T. Apostolova, P. M. Alsing, and D. A. Cardimona, to be published in Infr. Phys. & Tech. (2005).
9. T. W. Ebbesen, H. J. Lezec, H. F. Ghaemi, T. Thio, and P. A. Wolff, Nature (London) **391**, 667 (1998); H. F. Ghaemi, T. Thio, D. E. Grupp, T. W. Ebbesen, and H. J. Lezec, Phys. Rev. B **58**, 6779 (1998).
10. U. Schroter and D. Heitmann, Phys. Rev. B **58**, 15419 (1998).
11. R. Dragila, B. Luther-Davies, and S. Vukovic, Phys. Rev. Lett. **55**, 1117 (1985)
12. D. H. Huang, Y. Zhu, and S. X. Zhou, J. Phys.: Condens. Matter **1**, 7619 (1989).
13. D. H. Huang, C. Rhodes, P. M. Alsing, and D. A. Cardimona, submitted to JOSA B (2005).
14. D. H. Huang, Phys. Rev. B **53**, 13645 (1996).